TECHNICAL PAPER

ENHANCED TURBULENCE MODELING IN SOLIDWORKS FLOW SIMULATION

OVERVIEW

SolidWorks® Flow Simulation is a powerful, intelligent, and easy-to-use computational fluid dynamics (CFD) program that facilitates the work of product engineers who use SolidWorks 3D CAD software for 3D design creation. This paper details the approach and theory behind turbulence modeling as used in SolidWorks Flow Simulation to simulate complex industrial turbulent flows with heat and mass transfer. Detailed explanations and examples will support how SolidWorks Flow Simulation's turbulence model coupled with the immersed boundary Cartesian meshing techniques allow for accurate flow field resolution and enable Flow Simulation to offer a best-in-class CFD solution.

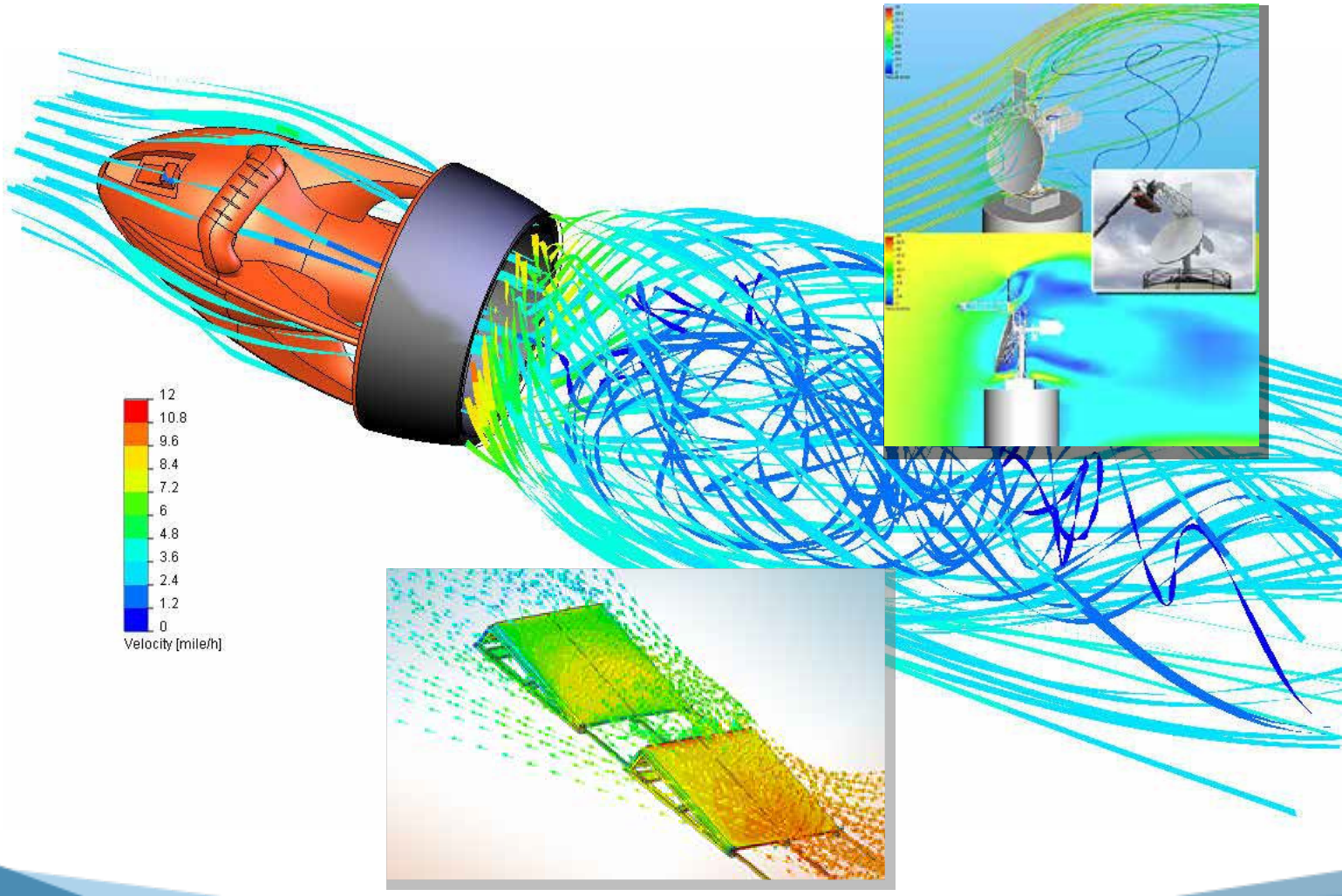

HAWK RIDGE SYSTEMS

SOLIDWORKS

INTRODUCTION

Today, product lifecycle management concepts (PLM) are widely deployed by engineers in many industries as the means by which 3D manufactured product data are used and maintained consistently during an entire product's lifecycle and across all its design changes. The basis of a PLM concept is the availability of high-quality, complete, detailed, and accurate 3D product model data within a CAD system as the central element. 3D product model data are therefore both the foundation and starting point for all virtual prototyping and physical simulations today. The use of fluid flow simulations (or Computational Fluid Dynamics, CFD) in such a CAD- embedded context is obviously very attractive as it can not only accelerate the design process, but it can make these processes more predictable and reliable, against a background of increasing design complexity and dependence on external development partners.

The systematic search for the best solution for a design is the objective of most CFD simulations and CFD software packages. The main criterion for flow and heat transfer simulation as an integral part of a PLM concept is efficient turnaround of high-quality CFD solutions, from geometry changes to resultant engineering interpretation in order to keep pace with design changes. To make CFD usable for mechanical designers and design engineers from other engineering disciplines, SolidWorks Flow Simulation is the unique SolidWorks-embedded general purpose concurrent CFD software package largely automated to minimize the specialist expertise required to operate traditional CFD software. The capabilities required for CAD-embedded CFD to not only handle very complex geometries without simplification, but also to simulate complex industrial turbulent flows with heat and mass transfer is very important, together with benchmarking SolidWorks Flow Simulation's turbulence capabilities against some classic industrial CFD validation cases.

SolidWorks Flow Simulation is a mature code with over 10 years of commercial presence and a thousand man-years of development effort behind it (Gavriliouk, 1993). It utilizes a modified k-E two-equation turbulence model designed to simulate accurately a wide range of turbulence scenarios in association with its pioneering immersed boundary Cartesian meshing techniques that allow for accurate flow field resolution with low cell mesh densities. For more information on immersed boundary meshes see for instance Kalitzin and Iaccarino (2002) and their work at Stanford University with General Motors on this approach for generating fast turnaround times for CFD simulations in upfront engineering design studies.

Depending on the fluid being examined and the flow conditions being considered, any fluid flow situation can be viewed (Schlichting, 1959) as one of the following:

- Laminar (a smooth flow without any disturbances)
- Turbulent (a flow regime characterized by random three-dimensional vorticity and intensive mixing)
- Transitional between laminar and turbulent (an alternation between laminar and turbulent flow regions)

There are usually no difficulties involved with CFD codes in simulating laminar flows which have clear unique solutions. However, direct simulations of turbulent flows taking into account fluid volume fluctuations are practically impossible for industrial situations because of the small physical sizes involved and the wide spectra of velocity fluctuations that would require extremely fine computation meshes to resolve them, long

CPU times to simulate them, and large computer memory to store the data produced. Hence, industrial turbulent fluid flows are simulated today usually by considering their effect on the time-average fluid flow characteristics in the volume being considered via semiempirical models of turbulence that close the fundamental Navier-Stokes equations being solved (Wilcox, 1994). The classical two-equation k-E empirical model for simulating turbulence effects in fluid flow CFD simulation (Launder & Spalding, 1972 and Wilcox, 1994) is still widely used and considered reliable for most industrial CFD simulations and it requires the minimum amount of additional information to calculate the flow field. In SolidWorks Flow Simulation the k-E model is used with a range of additional empirical enhancements added to cover a wide range of industrial turbulent flow scenarios (such as shear flows, rotational flows). For instance, damping functions proposed by Lam and Bremhorst (1981) for better boundary layer profile fit when resolving boundary layers with computational meshes have been added (the LB k-E model).

In addition to turbulence modeling, when simulating flows it is also necessary to simulate fluid boundary layer effects near solid bodies or walls that can be difficult to resolve due to high velocity and temperature gradients across these near-wall layers. To solve the Navier-Stokes equations with a two-equation k-E turbulence model without resolving the near-wall fluid boundary layer would require a very fine computational mesh, hence a "wall function" approach had been proposed by Launder and Spalding (1972, 1974) to reduce mesh sizes. According to this now classic approach, the fluid wall frictional resistance and heat fluxes from the fluid to the wall are used to calculate the wall boundary conditions for solving the Navier- Stokes equations. Naturally, the main domain flow's physical properties will be those of the boundary layer's external boundary conditions.

In SolidWorks Flow Simulation, Van Driest's (1956) universal profiles are employed to describe turbulent boundary layers and two approaches (called "Two-Scale Wall Functions," 2SWF) have been devised to fit a fluid's boundary layer profile relative to the main flow's properties:

- When the fluid mass centers of the near-wall mesh cells are located inside the boundary layer, i.e., the physical fluid flow boundary layer is thick
- When the fluid mass centers of the near-wall mesh cells are located outside the boundary layer, i.e., the physical fluid flow boundary layer is thin

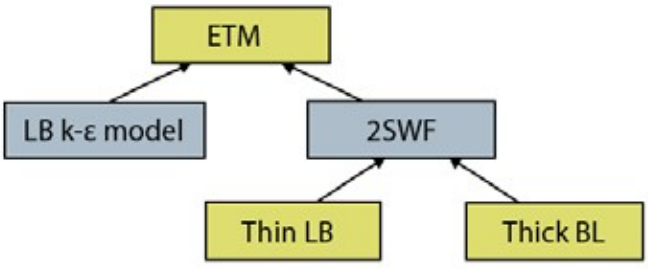

Figure 1. Structure of the ETM approach used in SolidWorks Flow Simulation CFD software

These two approaches allow SolidWorks Flow Simulation to overcome the traditional CFD code restriction of having to employ a very fine mesh density near the walls in the calculation domain and to use immersed boundary Cartesian meshes for all geometries (Kalitzin and Iaccarino, 2002).

Both the aforementioned SolidWorks Flow Simulation modification to the classical k-E turbulence model and the SolidWorks Flow Simulation modifications to the Launder-Spalding wall function approach for specifying the wall boundary conditions for the Navier-Stokes equations are called "Enhanced Turbulence Modeling" (ETM). Its structure is shown schematically in Figure1.

1. The SolidWorks Flow Simulation Modified k-E Turbulence Model

The modified k-E turbulence model with damping functions proposed by Lam and Bremhorst (1981) describes laminar, turbulent, and transitional flows of homogeneous fluids consisting of the following turbulence conservation laws:

$$\frac{\partial \rho k}{\partial t}+\frac{\partial \rho k u_i}{\partial x_i}=\frac{\partial}{\partial x_i}\left(\left(\mu+\frac{\mu_t}{\sigma_k}\right)\frac{\partial k}{\partial x_i}\right)+\tau_{ij}^R\frac{\partial u_i}{\partial x_j}-\rho\varepsilon+\mu_t P_B, \tag{1.1}$$

$$\frac{\partial \rho \varepsilon}{\partial t}+\frac{\partial \rho \varepsilon u_i}{\partial x_i}=\frac{\partial}{\partial x_i}\left(\left(\mu+\frac{\mu_t}{\sigma_\varepsilon}\right)\frac{\partial \varepsilon}{\partial x_i}\right)+C_{\varepsilon 1}\frac{\varepsilon}{k}\left(f_1\tau_{ij}^R\frac{\partial u_i}{\partial x_j}+C_B\mu_t P_B\right)-f_2 C_{\varepsilon 2}\frac{\rho\varepsilon^2}{k}, \tag{1.2}$$

$$\tau_{ij}=\mu\, s_{ij},\quad \tau_{ij}^R=\mu_t\, s_{ij}-\frac{2}{3}\rho k\delta_{ij}\ ,s_{ij}=\frac{\partial u_i}{\partial x_j}+\frac{\partial u_j}{\partial x_i}-\frac{2}{3}\delta_{ij}\frac{\partial u_k}{\partial x_k}, \tag{1.3}$$

$$P_B=-\frac{g_i}{\sigma_B}\frac{1}{\rho}\frac{\partial \rho}{\partial x_i}, \tag{1.4}$$

where $C_\mu=0.09$, $C_{\varepsilon 1}=1.44$, $C_{\varepsilon 2}=1.92$, $\sigma_k=1$, $\sigma_\varepsilon=1.3$, σ_B=0.9, $C_B=1$ if $P_B>0$, $C_B=0$ if $P_B<0$, the turbulent viscosity is determined from:

$$\mu_t=f_\mu\cdot\frac{C_\mu\rho k^2}{\varepsilon}, \tag{1.5}$$

Lam and Bremhorst's damping function f_μ is determined from:

$$f_\mu=\left(1-e^{-0.025R_y}\right)^2\cdot\left(1+\frac{20.5}{R_t}\right), \tag{1.6}$$

where

$$R_y=\frac{\rho\sqrt{k}y}{\mu}, \tag{1.7}$$

$$R_t=\frac{\rho k^2}{\mu\varepsilon}, \tag{1.8}$$

y is the distance from point to the wall and Lam and Bremhorst's damping functions f_1 and f_2 are determined from:

$$f_1=1+\left(\frac{0.05}{f_\mu}\right)^3,\quad f_2=1-e^{R_T^2}. \tag{1.9}$$

Lam and Bremhorst's damping functions ϕ_μ, ϕ_1, ϕ_2 decrease turbulent viscosity and turbulence energy and increase the turbulence dissipation rate when the Reynolds number Ry based on the average velocity of fluctuations and distance from the wall becomes too small. When $\phi_\mu = 1$, $\phi_1 = 1$, $\phi_2 = 1$ the approach obtains the original k-E model.

2. Two-Scale Wall Functions

The Two-Scale Wall Functions (2SWF) in SolidWorks Flow Simulation consist of two approaches to coupling the boundary layer calculation with the main flow properties:

- The thick-boundary-layer approach when $\beta > A \bullet y$
- The thin-boundary-layer approach when $\beta \le A \bullet y$

where β is the boundary layer thickness, y is the distance from the near-wall computational mesh cell's fluid mass center to the wall (Figure 2), and $A \ge 1$ is a coefficient depending on flow conditions.

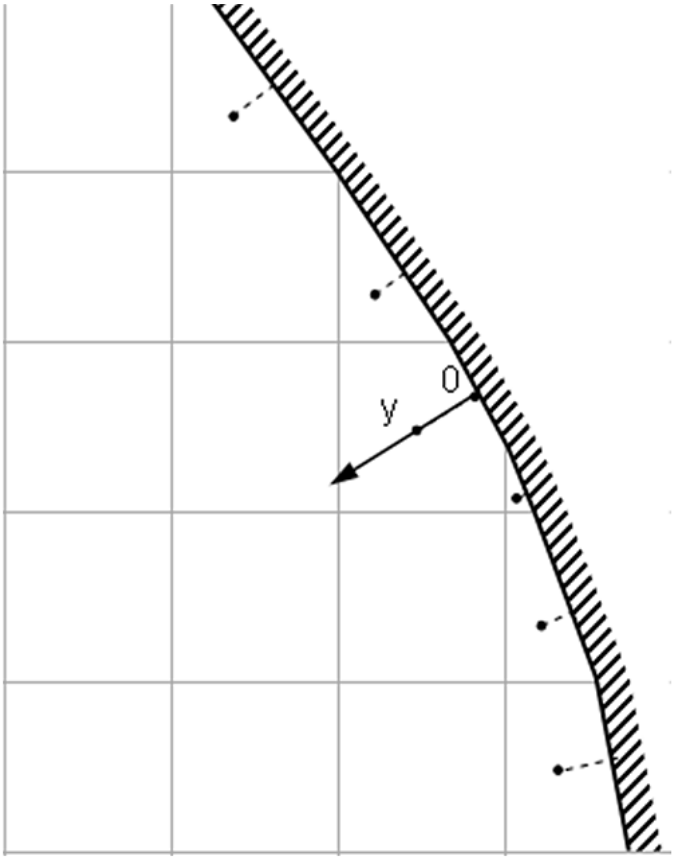

Figure 2. Computational mesh cells near a wall, their fluid mass centers, and the distances from them to the wall (dashed lines)

2.1 The Thick-Boundary-Layer Approach

When a fluid's boundary layer thickness, $\beta > A \bullet y$, where y is the distance from the near-wall computational mesh cell's fluid mass center to the wall (Figure 2), and $A \ge 1$ is a coefficient depending on flow conditions,

that is, the near-wall computational mesh cell's fluid mass center is located inside the boundary layer. Instead of y, SolidWorks Flow Simulation uses the dimensionless $y^+ = \frac{\sqrt{\rho\tau_w}\,y}{\mu}$. Since the computational mesh used in SolidWorks Flow Simulation is always an immersive boundary non-body-fitted Cartesian mesh, y^+ of some near-wall cells could be very small (Figure 2). Hence, the corresponding dimensionless distance from the turbulent equilibrium region's outer boundary to the wall follows from an analysis of the experimental data presented by Wilcox (1994) and is equal to $y_{UP}^+ = 300$. With this approach SolidWorks Flow Simulation obtains the momentum, heat flux, and turbulent boundary conditions for the Navier-Stokes equations which are described below.

2.2 The Momentum Boundary Condition

Since $y^+ < y_{UP}^+$ and proceeding from the Van Driest mixing length (1956), the dimensionless longitudinal velocity $u^+ = \frac{u}{\sqrt{\frac{\tau_w}{\rho}}}$ in the boundary layer depends on the dimensionless y^+ in the following manner:

$$u^+ = \int_0^{y^+} \frac{2 \cdot d\eta}{1 + \sqrt{1 + 4 \cdot \kappa^2 \cdot \eta^2 \cdot \left[1 - \exp\left(-\frac{\eta}{A_v}\right)\right]^2}}$$, (2.1)

where $K = 0.4054$ is the Karman constant, $A_v = 26$ is the Van Driest coefficient.

The wall shear stress being the momentum boundary condition governing the fluid velocity u at the near-wall computational mesh cell's center is determined as , $\tau_w = \frac{\mu \cdot u}{y} \cdot K$, (2.2) where $K = K(y^+)$ is a correction coefficient determined from equation (2.1) and the function $u^+ = u^+(K(y^+))$.

In SolidWorks Flow Simulation an equivalent sand wall roughness k_s is taken into account by adding $u_{DEF}^+(k_S^+)$ function in equation (2.1):

$$u^+ = u_{def}^+ + \int_0^{y^+} \frac{2 \cdot d\eta}{1 + \sqrt{1 + 4 \cdot \kappa^2 \cdot \eta^2 \cdot \left[1 - \exp\left(-\frac{\eta}{A_v}\right)\right]^2}},$$, (2.3) where u_{DEF}^+ is a dimensionless function of the dimensionless roughness height $k_s^+ = \frac{\sqrt{\rho\tau_w}\,k_s}{\mu}$, where k_s is the physical roughness height. The $u^+_{DEF}(k_S^-)$ function has been determined from the experimental data obtained in flow over a flat plate (Wilcox, 1994) and the boundary condition $u^+_{DEF}(k_S = 0) = 0$. Correspondingly, $K = K(y^+, k_S^+)$.

If $\mathrm{Re}_\delta = \frac{\rho u^e \delta}{\mu}$, < 4000, where u^e is the fluid flow velocity at the boundary layer's fluid boundary, i.e., at the distance of the boundary layer thickness β from the wall, the boundary layer is considered to be laminar, so $K = 1$.

2.3 The Heat Flux Boundary Condition

The heat flux across the boundary layer can be determined $q = C_p\left(\frac{\mu}{\mathrm{Pr}} + \frac{\mu_t}{\mathrm{Pr}_t}\right)\frac{\partial T}{\partial y}$ from . (2.4).

Since it is constant along the y direction, the heat flux from the fluid to the wall is the heat transfer boundary condition governing the fluid temperature T at the near- wall computational mesh cell's center and it can be determined from $q_w = \lambda\frac{T - T_w}{y}\cdot K\cdot\Phi$ (2.5) where K is described in the previous section, and $\Phi = \Phi\left(y^+, \frac{\mathrm{Pr}}{\mathrm{Pr}_t}\right)$ is determined from equation (2.4).

In the same manner as in the previous section, if Re_β, the boundary layer is considered to be laminar, so $K = 1$, $<I = 1$.

2.4 Turbulence Boundary Conditions

The turbulence boundary conditions for k and E depend on where the near-wall computational mesh cell's fluid mass center is located: in the turbulence equilibrium region or nearer to the wall. If it is located in the turbulence equilibrium region, i.e., $y^+ > 30$, then at the near-wall computational mesh cell's fluid mass center.

$$\frac{\partial k}{\partial y} = 0, \quad \varepsilon = \frac{C_\mu^{0.75} k^{1.5}}{\kappa y} \quad (2.6)$$

If $y^+ \le 30$, i.e., the near-wall computational mesh cell's fluid mass center is located in the turbulence nonequilibrium region, then at this cell's fluid mass center, $k^+ = k^+(y^+), \quad \varepsilon^+ = \varepsilon^+(y^+)$ (2.7) which had been determined from experimental data obtained on a plate (Lapin, 1982).

2.5 The Thin-Boundary-Layer Approach

In the thin-boundary-layer approach the Prandtl boundary layer equations already integrated along the normal-to-the-wall (i.e., along the y ordinate) from 0 (at the wall) to the boundary layer thickness b are solved along a fluid streamline near the wall. If the boundary layer is laminar, these equations are solved in SolidWorks Flow Simulation with a method of successive approximations based on the Shvetz trial functions technology (Ginzburg, 1970). If the boundary layer is turbulent or transitional (between laminar and turbulent), SolidWorks Flow Simulation uses a generalization of this method to such boundary layers employing the Van Driest hypothesis about the mixing length in turbulent boundary layers (1956).

Three-dimensional effects of fluid flow over concave and convex surface walls, i.e., fluid spilling or collecting near such walls, are taken into account inside SolidWorks Flow Simulation through corresponding corrections for the wall curvature. Flow and boundary layer separations are also determined with a special method in SolidWorks Flow Simulation taking the near-zero wall shear stress into account. The equivalent sand wall roughness and the external flow's turbulence on the boundary layer are taken into account through semiempirical coefficients correcting the wall shear stress and the heat flux from the fluid to the wall in SolidWorks Flow Simulation.

Fluid compressibility, turbulence kinetic energy dissipation, and various mass forces are also taken into account through corresponding empirical and semi- empirical models.

From the boundary layer calculation SolidWorks Flow Simulation obtains the boundary layer thickness b the wall shear stress 1_w:^{e}, and the heat flux from the fluid to the wall q_w^e, which are used as boundary conditions for the Navier-Stokes equations, which are described below.

2.6 The Momentum and Heat Flux Boundary Conditions

The momentum and heat flux boundary conditions are written as $\tau_w = \tau_w^e, \quad q_w = q_w^e$, (2.8).

2.7 Turbulence Boundary Conditions

Turbulence boundary conditions for *k* and E are determined from the condition of turbulence equilibrium in the near-wall computational mesh cell: $\frac{\partial k}{\partial y} = 0, \qquad \varepsilon = \frac{C_\mu^{0.75} k^{1.5}}{\kappa y}$ (2.9).

3. Benchmark CFD Turbulence Validations with SolidWorks Flow Simulation

Several classical CFD turbulence benchmark examples are presented here to demonstrate the following:

- SolidWorks Flow Simulation's accuracy in calculating a wide region of Reynolds numbers on the immersed boundary Cartesian computational meshes used in SolidWorks Flow Simulation
- SolidWorks Flow Simulation results with refinement of the immersed boundary computational mesh

3.1 Flow over a Flat Plate

Consider an airflow of u_∞=20 m/s velocity over a smooth flat plate of 0.5 m length (Figure 3).

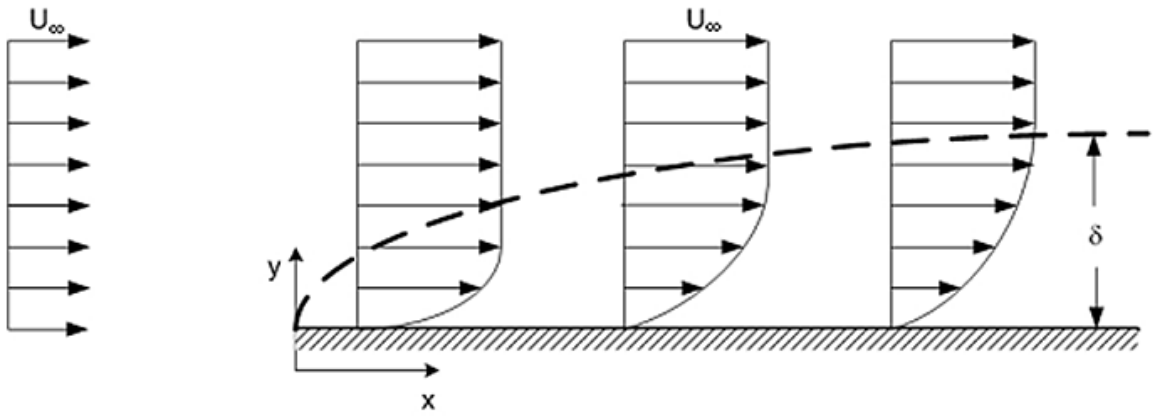

Figure 3. Schematic representation of boundary layer development on a flat plate

SolidWorks Flow Simulation predictions for a computational mesh of 200×50 cells of the obtained fluid velocity field are shown in Figure 4.

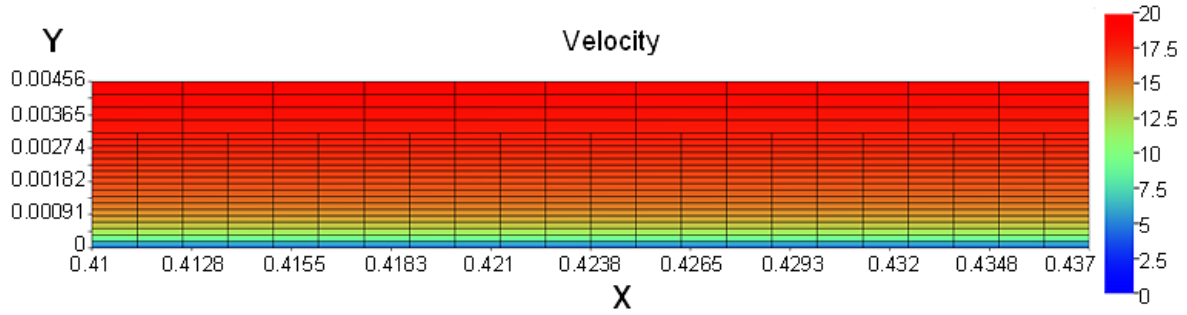

Figure 4. Computational mesh and the resultant velocity distribution at z=0 (zoom-view)

CFD simulation results obtained in SolidWorks Flow Simulation on a similar computational mesh of 200×100 cells with a varying incoming flow's turbulence intensities of Tu=0.5%, 0.8%, 1.0%, 1.25%, 1.5%, 2.0% are presented in Figures 5, 6, and 7. In these calculations $y^+ \approx 6$ in the turbulent region, so the boundary layer's laminar sublayer is not being resolved by the computational mesh.

Taking the SolidWorks Flow Simulation-calculated local flat plate friction coefficient: $C_f = \frac{\tau_w}{0.5\rho u_\infty^2}$ (4.1)

for these cases and plotting it versus the Reynolds number in comparison with the Blasius semiempirical law (Schlichting, 1979) for the laminar boundary layer (on the plate's inlet section): $C_f = \frac{0.664}{\sqrt{\mathrm{Re}_x}}$ (4.2). and

the Prandtl-Schlichting semiempirical law (Schlichting, 1979) for the turbulent boundary layer (on the plate's following section). The results are presented in Figure 5:

$$C_f = \left(2\lg \mathrm{Re}_x - 0.65\right)^{-2.3} \quad (4.3)$$

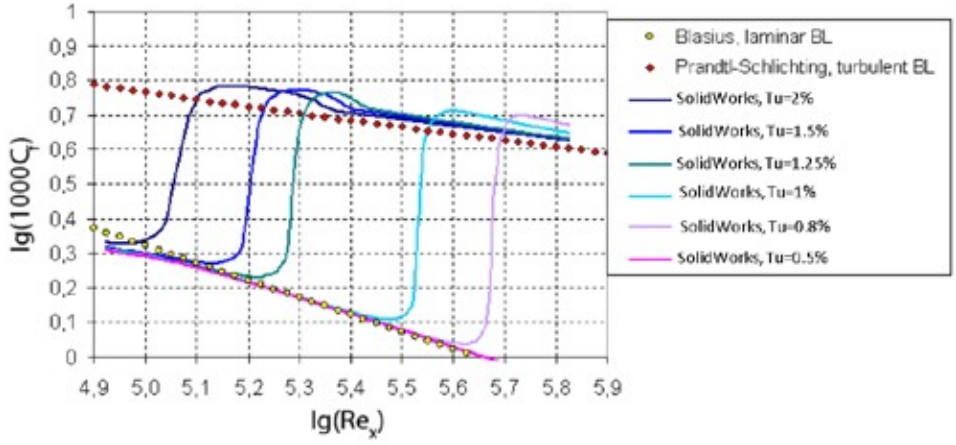

Figure 5. The smooth flat plate's local friction coefficient calculated with SolidWorks Flow Simulation and for comparison with the Blasius and Prandtl-Schlichting formulae (Schlichting 1979)

In the SolidWorks Flow Simulation calculations, the minimum Re_x, at which the boundary layer is laminar for any incoming flow turbulence intensity, is close to the experimental value of $Re_x = 6 \cdot 10^4$ (Schlichting, 1979), and the SolidWorks Flow Simulation-calculated maximum Re_x, at which the boundary layer is turbulent at any incoming flow turbulence intensity, is close to the experimental value of $Re_x = 3 \cdot 10^6$ (Schlichting, 1979).

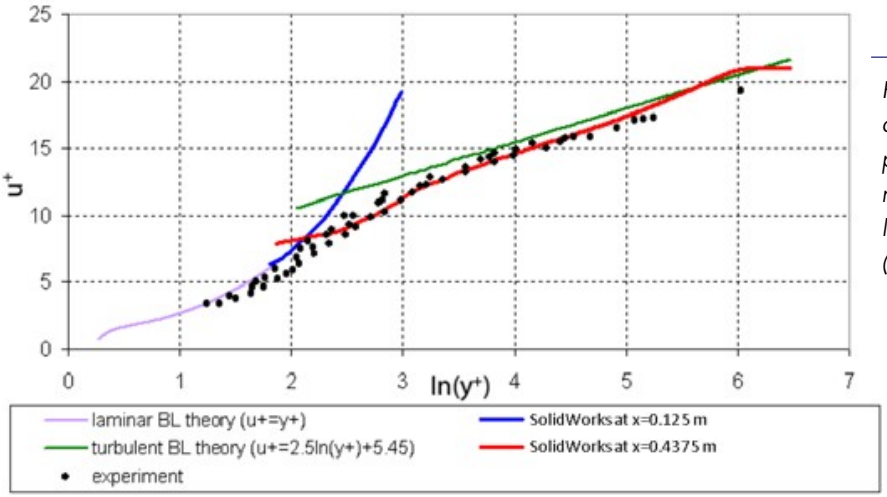

Figure 6. The flat plate boundary layer velocity profiles calculated with SolidWorks Flow Simulation on the flat plate inlet section with laminar boundary layer (x=0.125 m), on the flat plate exit section with turbulent boundary layer (x=0.4375 m) in comparison with experimental data (Ref. 2) and semiempirical theory (Schlichting, 1979)

The SolidWorks Flow Simulation-calculated local Nusselt number dependences $Nu_x(Re_x)$ at the different incoming flow turbulence intensities with the semiempirical dependences for airflows over flat plates (Pr=0.72) with laminar (4.4) and turbulent (4.5) boundary layers is shown in Figure 7:

$$Nu_x = 0.332 \cdot Re_x^{1/2} Pr^{1/3}, \quad (4.4)$$

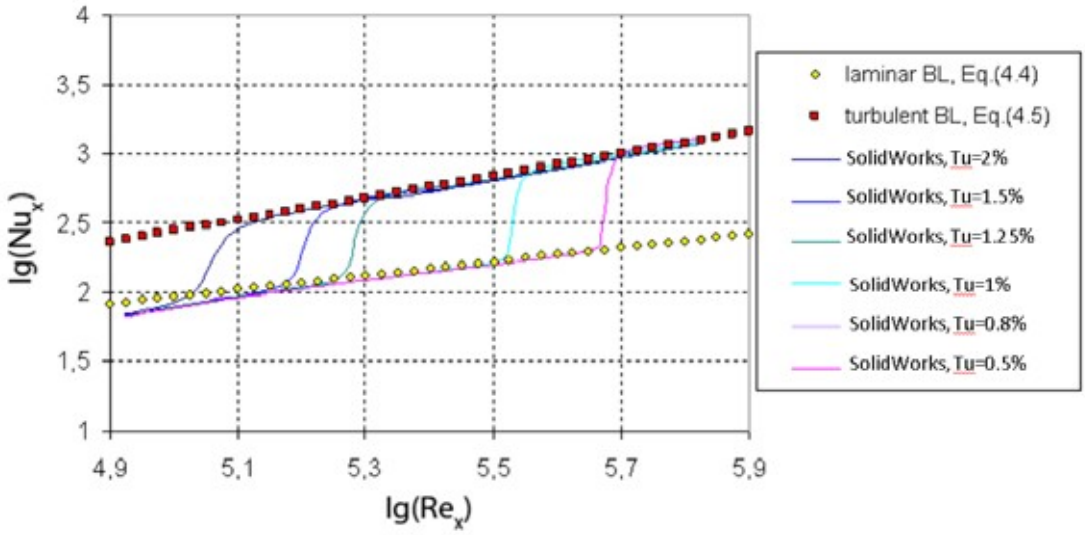

$$Nu_x = 0.032 \cdot Re_x^{0.8} Pr^{0.43}, \quad (4.5)$$

Figure 7. The local Nusselt number of airflow over a smooth flat plate vs. calculated with SolidWorks Flow Simulation and, for comparison, with the semiempirical equations (4.4) and (4.5) (Lienhard and Lienhard, 2004)

3.2 Couette flow between Two Parallel Flat Plates at Re=3.4 x10^4

A classical plane flow is one between two parallel infinite flat plates spaced at a distance *h* from one another and moving at velocity U in opposite directions (Figure 8), resulting in the flow Reynolds number, $\frac{Re=\pi Uh}{\mu=3.4x10^4}$

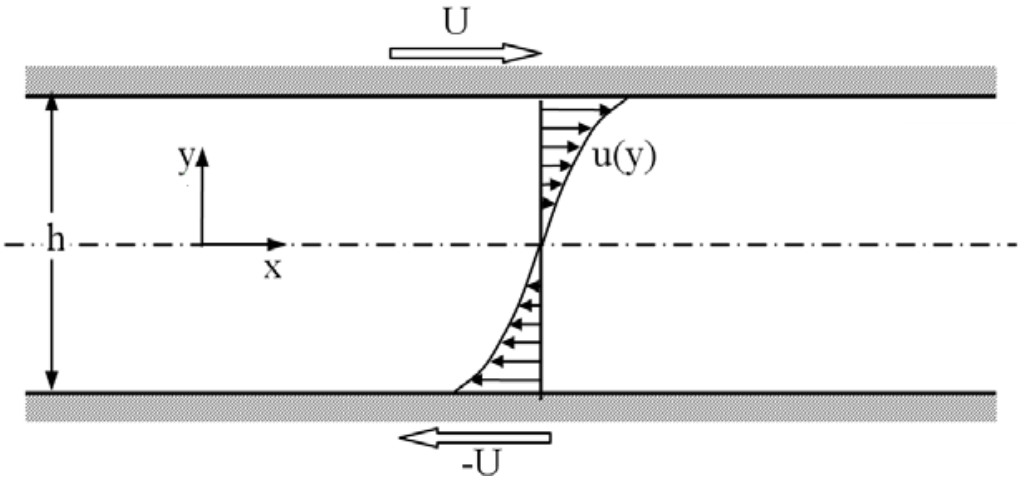

Figure 8. A turbulent Couette flow between two parallel plates moving in opposite directions

Dimensionless velocity profiles calculated within SolidWorks Flow Simulation for different computational meshes (10, 20, 40, 80 mesh cells across the channel) in comparison with experimental data (Schlichting, 1979) are shown in Figure 9.

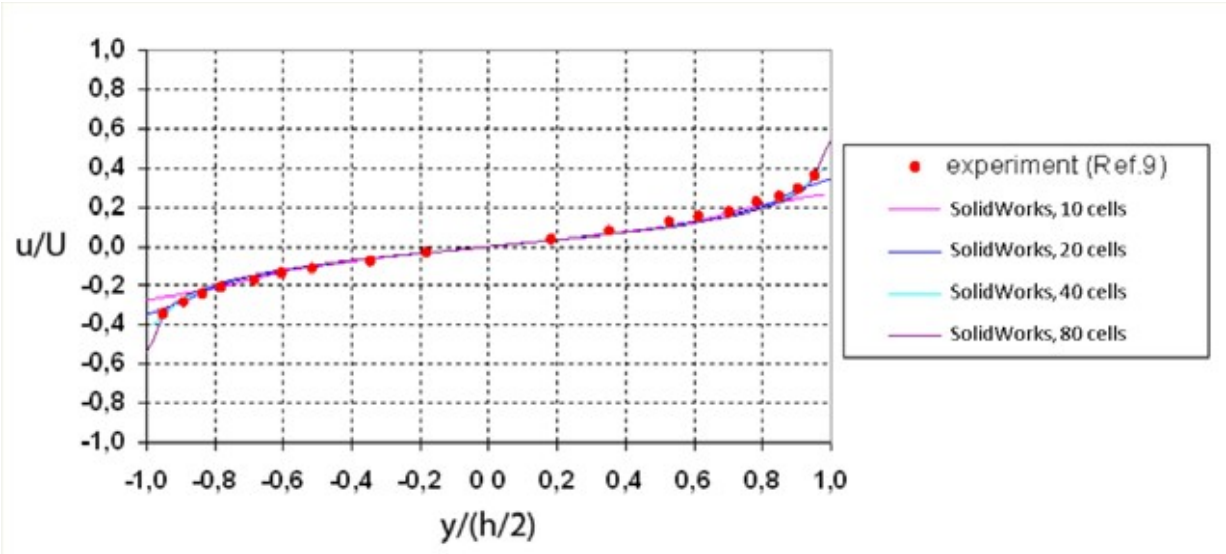

Figure 9. SolidWorks Flow Simulation-calculated dimen-sionless velocity profiles of turbulent Couette flow bet-ween two parallel plates moving in opposite directions in comparison with the experimental data (Schlichting, 1979)

We can see good agreement between the SolidWorks Flow Simulation calculations with the experimental data: y^+ =75 for the 10-cells mesh, y^+ =37.5 for the 20-cells mesh, y^+ =19 for the 40-cells mesh, and y^+ =9.5 for the 80 cells mesh showing how robust the solver is with coarse meshes.

3.3 Flow over a Backward-Facing Step at Re=5,000

Consider airflow in a rectangular channel having parallel walls (Hirsch, 1988), 1.0 m length × 15.1 cm width × Y_0=10.1 cm height as the inlet section, and an H=1.27 cm height backward-facing step on the bottom of the domain (Figure 10). Due to the channel's large aspect ratio (the tunnel-width to step-height ratio is equal to 12), three-dimensional effects in the flow separation region downstream of the backward-facing step are minimal, and due to the channel's small expansion ratio $(Y_0 + H)/Y_0 = 1.125$, the pressure gradient downstream of the sudden expansion is also at a minimum.

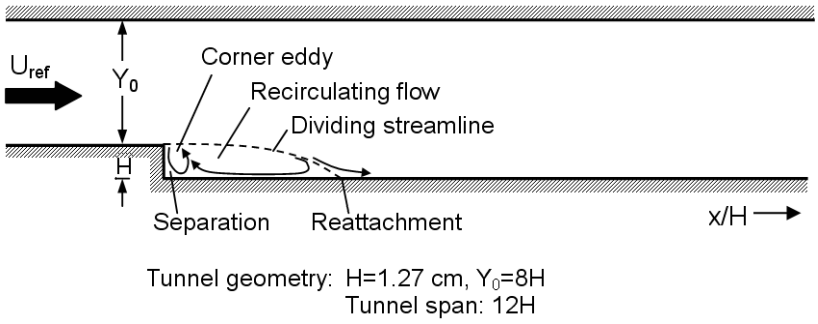

Figure 10. Flow in a rectangular channel with parallel walls and a backward-facing step on the bottom

At a distance 4H upstream of the backward-facing step, the inlet airflow has a velocity of 44.2 m/s, the atmospheric total pressure and temperature—this flow's Mach number is equal to 0.128—and the fully turbulent boundary layer of 1.9 cm thickness provided by the high Reynolds number of 5,000 (based on the boundary layer momentum thickness).

SolidWorks Flow Simulation calculations of this flow were performed on uniform computational meshes having 10, 20, and 40 cells per the step height (Figure 11).

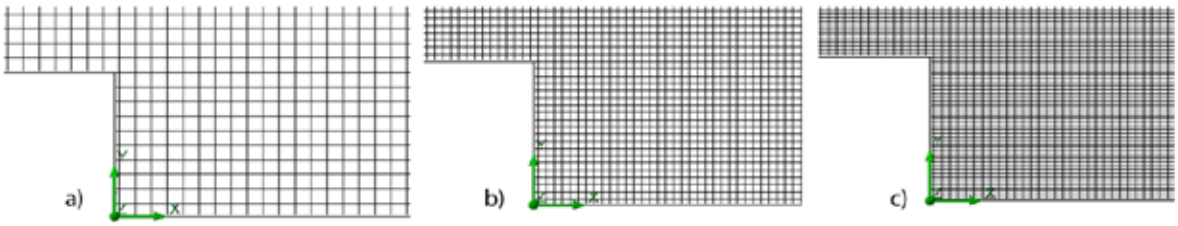

Figure 11. The SolidWorks Flow Simulation computational meshes of different density used: the number of cells traversing the step height: a) 10 cells, b) 20 cells, c) 40 cells

SolidWorks Flow Simulation-calculated flow velocity profiles, wall friction downstream of the backward-facing step, and the separated flow reattachment's distance from the backward-facing step are presented in Figs.12 and 13 and in Table 1. In these calculations y^+ = 0 up to 54 in the computational mesh of 10 cells per step height, H, y^+ = 0 up to 27 at the computational mesh of 20 cells per H, and y^+ = 0 up to 13 at the computational mesh of 40 cells per H. Good convergence of these SolidWorks Flow Simulation calculation results with the computational mesh refinements chosen and good agreement of these results with the experimental data (Driver and Seegmiller, 1985) and calculations (Wilcox, 1994).

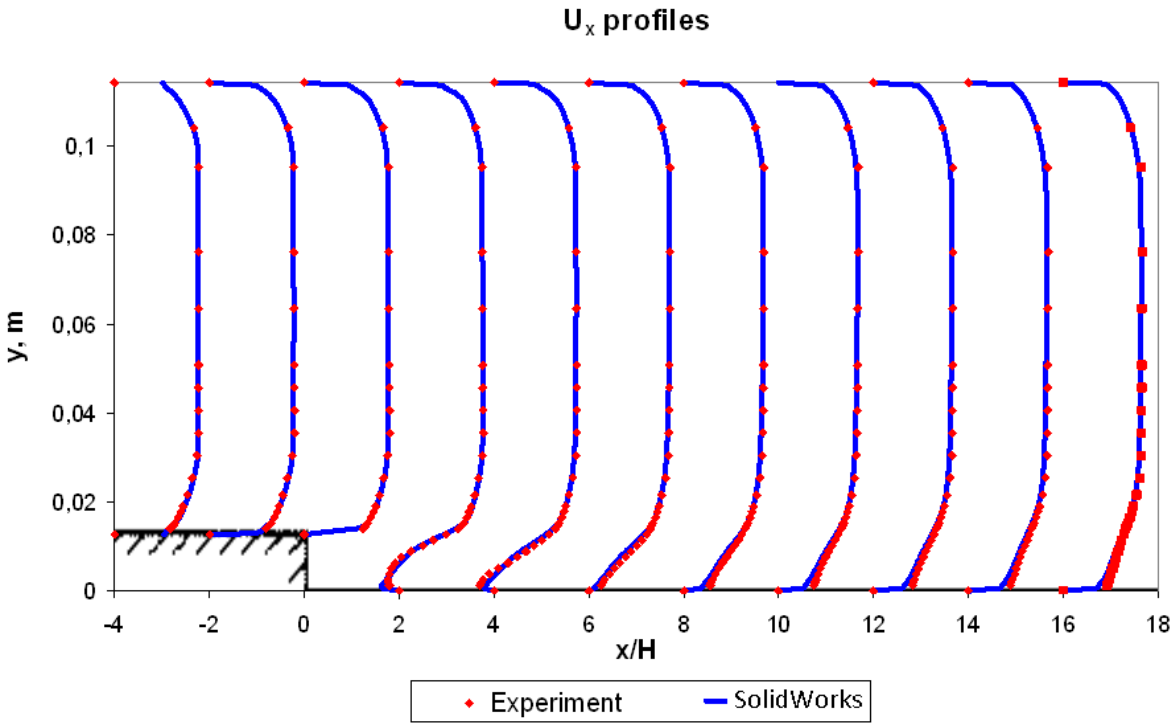

Figure 12. SolidWorks Flow Simulation-calculated flow velocity profiles obtained with the computational mesh of 10 cells per step height in comparison with experimental data (Driver and Seegmiller, 1985)

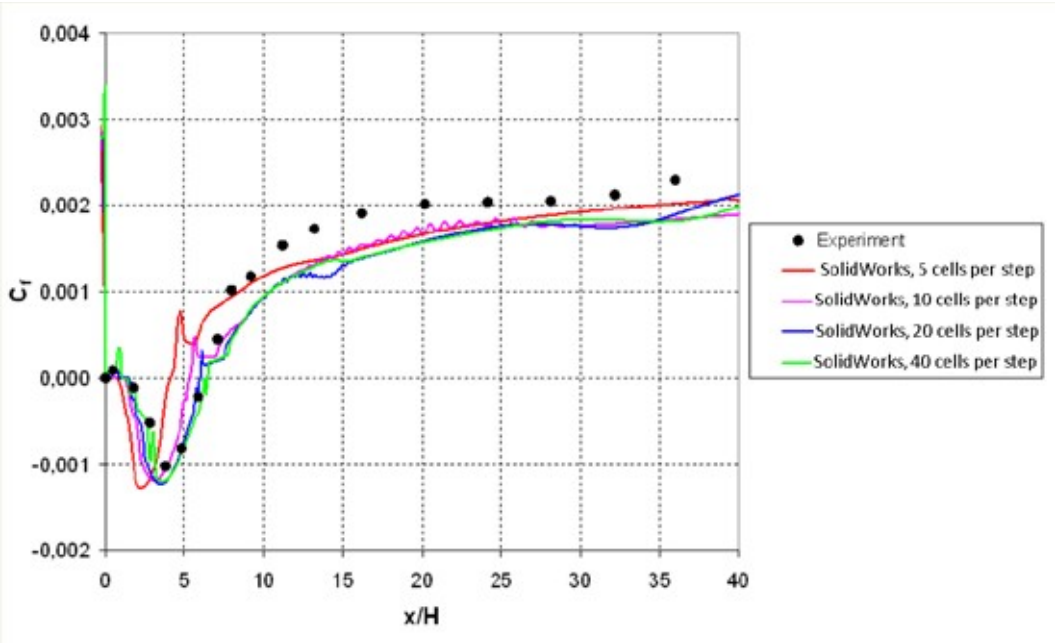

Figure 13. The SolidWorks Flow Simulation-calculated wall friction coefficient of the flow past the back step in comparison with experimental data (Driver and Seegmiller, 1985)

Table 1 SolidWorks Flow Simulation-calculated distance of the separated flow reattachment point downstream of the backward facing step in comparison with experimental data (Driver and Seegmiller 1985) and calculations (Wilcox 1994).

	x/H	Deviation from experimental data (%)
Experiment (Driver and Seegmiller 1985)	6.2	0
SolidWorks Flow Simulation, 10 cells per H	5.37	-13
SolidWorks Flow Simulation, 20 cells per H	6.00	-3
SolidWorks Flow Simulation, 40 cells per H	6.27	1
Calculation with the k-E model (Wilcox 1994)	5.2	-16
Calculation with the k-μ model (Wilcox 1994)	6.4	3

3.4 Flow over a Cylinder at Re=3.7x10^5

Consider unsteady airflow over a circular cylinder at the incoming airflow velocity of 153 m/s under normal pressure and temperature at the cylinder-diameter-based Reynolds number of Re=3.7x10^5. SolidWorks Flow Simulation calculations were then carried out with computational mesh densities having 20, 40, and 80 cells per cylinder diameter. In all these calculations the thin-boundary-layer turbulence model was employed.

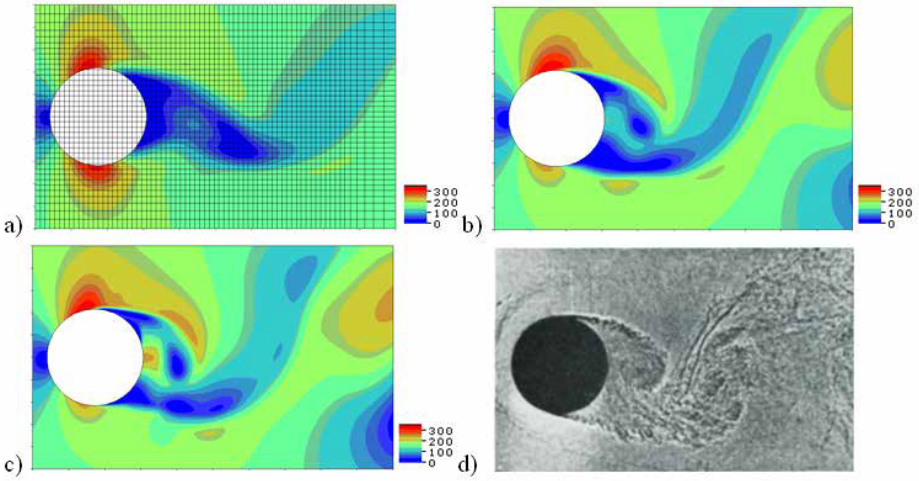

The computational mesh and results for 20 cells per cylinder diameter is shown in Figure 14a. SolidWorks Flow Simulation-calculated velocity fields and an experimental shadowgraph (Driver and Seegmiller 1985) of real flow over a circular cylinder at nearly the same Reynolds number are shown in Figure 14.

Figure 14. Predicted flow velocity fields over a circular cylinder, calculated with SolidWorks Flow Simulation for different computational meshes having a) 20 cells per diameter, b) 40 cells per diameter, c) 80 cells per diameter, and, d) similar real flow shadowgraph from Driver and Seegmiller (1985)

The drag coefficient, C_d, of the cylinder calculated with SolidWorks Flow Simulation for the different computational meshes in comparison with experimental data (Driver and Seegmiller 1985), as well as the corresponding y^+ values, are presented in Table 2.

Table 2 Circular cylinder drag coefficients calculated with SolidWorks Flow Simulation in comparison with experimental data (Driver and Seegmiller 1985).

Mesh density (cells per cylinder diameter)	C_d	Deviation from the Ref.12 experimental data (%)	y^+_{max}
SolidWorks Flow Simulation, 20 cells per diameter	0.82	-18	650
SolidWorks Flow Simulation, 40 cells per diameter	0.95	-5	330
SolidWorks Flow Simulation, 80 cells per diameter	1.02	2	170
Experiment (Driver and Seegmiller 1985)	1.0	0	n/a

The SolidWorks Flow Simulation simulation predictions for varying computational mesh densities shows very good agreement with the experimental data from Driver and Seegmiller (1985).

3.5 Flow over a Generic Car Body Shape (the Ahmed Body)

A classical automotive external aerodynamics wind tunnel test case is the so-called "Ahmed Body" (Lienhart, Stoots, and Becker, 2000) which has a curved, chamfered front end, box-like main body and sloping rear section. Using SolidWorks Flow Simulation, an approaching airflow of 40 m/s on the generic model car body of 1,044 mm length, 389 mm width, and 288 mm height and mounted in a wind tunnel of 1,870 mm × 1,400 mm cross-section at a 50 mm height above the floor on 4 stilts of 30 mm diameter was created—see Figure 16. The model car body's slanting rear section of 222 mm length was modeled with different (35° and 25°) slant angles.

In the experimental study, flow had started to separate from the body's slanting surface at an angle of 30°. The flow's Reynolds number based on the body height and the incoming flow velocity is equal to Re = 7.68×10^5. SolidWorks Flow Simulation calculations were performed with a computational mesh of 209 cells in length, 58 cells in height, and 78 cells in width to resolve the car body (Figure 15).

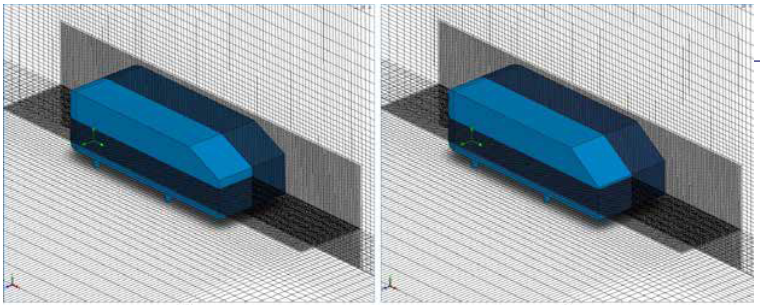

Figure 15. The SolidWorks Flow Simulation computational mesh over the model car body: a) the 25° rear slant, b) the 35° rear slant

SolidWorks Flow Simulation-calculated flow streamlines and velocity contours upstream, over, and downstream of the model car body are shown in Figure 16 for the two sloping rear slant angles. The SolidWorks Flow Simulation-calculated flow velocity profiles and body drag coefficients in comparison with the experimental ones (Lienhart, Stoots, and Becker, 2000) are shown in Figure 17 and Table 3. It can be seen from Figs.16 and 17 that in the SolidWorks Flow Simulation calculations the flow over the body is attached to the body's slanting rear surface if it has the 25° rear slant angle and separates from this surface if it has the 35° angle, and the calculated flow velocity profiles are close to the experimental ones. From Table 3 it is observed that the SolidWorks Flow Simulation-calculated body drag coefficients agree well with the experimental ones.

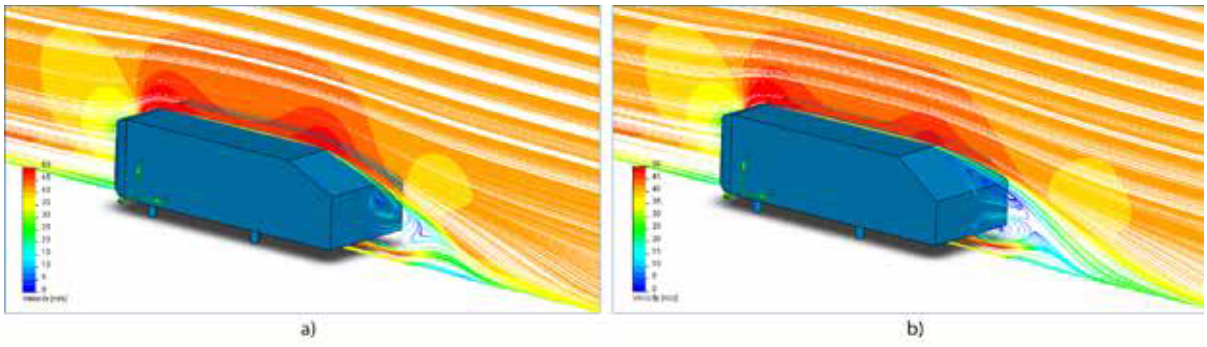

Figure 16. SolidWorks Flow Simulation-calculated flow streamlines and velocity contours upstream, over, and downstream of the model car body: a) the 25° body slant, b) the 35° body slant

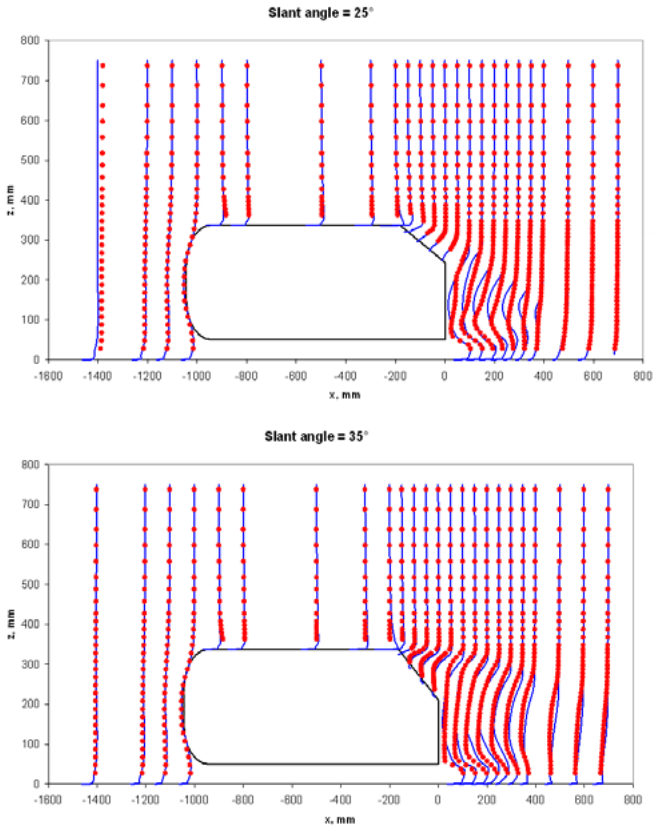

Figure 17. SolidWorks Flow Simulation-calculated flow velocity profiles in the body's symmetry plane in comparison with experimental data at the body's slant angles of 25° and 35° degrees: – SolidWorks Flow Simulation calculation, ˍ experiment (Lienhart, Stoots, and Becker, 2000)

Table 3 The model car body's drag coefficient calculated with SolidWorks Flow Simulation and obtained in wind tunnel experiments (Lienhart, Stoots, and Becker, 2000)

Ahmed body's slant angle	$C_{d,\ exp}$	$C_{d,\ SolidWorks}$	Deviation from the Ref. 13 experimental data (%)	y^+_{max} on the slanted surface
25°	0.298	0.284	-4.8	1401
35°	0.257	0.274	6.6	1402

CONCLUSIONS

The general purpose SolidWorks-embedded CFD solver in the SolidWorks Flow Simulation software package has been benchmarked against a wide range of CFD turbulence cases and its two-equation modified k-E turbulence model with its unique two-scale wall functions approach and immersed boundary Cartesian meshes leads to good predictions for spatial laminar, turbulent, and transitional flows over a range of compressible and anisotropic flows. Boundary layer resolution was good in all cases even though mesh densities were varied and coarse by traditional CFD approaches and the determination of wall friction and heat fluxes from the fluid flow to the wall interface over a wide range of Reynolds numbers was excellent.

REFERENCES

Driver, D.M. and Seegmiller, H.L., 1985. Features of a Reattaching Turbulent Shear Layer in Divergent Channel Flow. *AIAA Journal*, Vol. 23, p. 163

Gavriliouk, V.N., Denisov, O.P., Nakonechny, V.P., Odintsov, E.V., Sergienko, A.A., Sobachkin, A.A., 1993. Numerical Simulation of Working Processes in Rocket Engine Combustion Chamber. *44th Congress of the International Astronautical Federation*, IAF-93-S.2.463, October 16-22, Graz, Austria

Ginzburg, I. P., 1970. Theory of Drag and Heat Transfer. Leningrad, LGU (in Russian)

Griffiths, W.D., and Boysan, F., 1996. Computational fluid dynamics (CFD) and empirical modelling of the performance of a number of cyclone samplers, *Journal of Aerosol Science*, Vol. 27, No. 2, pp. 281-304

Hirsch, C., 1988. Numerical Computation of Internal and External Flows, Volume I, *Fundamentals of Numerical Discretization*. New York: John Wiley & Sons

Kalitzin, G., and Iaccarino, G., 2002. Turbulence Modeling in an Immersed-Boundary RANS-Method, Center for Turbulence Research Annual Research Briefs, Stanford University, California, pp. 415 - 426

Lam, C.K.G. and Bremhorst, K.A., 1981. Modified Form of Model for Predicting Wall Turbulence. *ASME Journal of Fluids Engineering*, Vol. 103, pp. 456-460

Lapin, Y.V., 1982. Turbulent Boundary Layer in Supersonic Gas Flows. Moscow, Nauka, (in Russian)

Launder, B.E. and Spalding, D.B., 1972. Lectures in Mathematical Models of Turbulence. Academic Press, London, England.

Launder, B. E. and Spalding, D. B. The Numerical Computation of Turbulent Flows. *Computer Methods in Applied Mechanics and Engineering*, Vol. 3, 1974, pp. 269-289

Lienhard IV, J.H. and Lienhard V, J.H., 2004. A Heat Transfer Textbook. 3rd ed., Cambridge, MA: Phlogiston Press

Lienhart, H., Stoots, C., Becker, S., 2000. Flow and turbulence structures in the wake of a simplified car model (Ahmed model). DGLR Fach Symp. der AG STAB, Stuttgart University

Mentor Graphics Corp., 2011. Advanced Immersed Boundary Cartesian Meshing Technology in SolidWorks Flow Simulation

Schlichting, H., 1959. *Entstehung der Turbulenz*. Berlin (in German)

Schlichting, H., 1979. *Boundary-Layer Theory*. McGraw-Hill, New York

Van Driest, E.R., 1956. On Turbulent Flow Near a Wall. *Journal of the Aeronautical Sciences*, Vol. 23, No. 10, p. 1007

Wilcox, D.C., 1994. *Turbulence Modeling for CFD*. DCW Industries

NOMENCLATURE

u_i – *i*-th component of the fluid velocity vector

π – fluid density

k – turbulence energy

E – dissipation rate of turbulence energy

μ – fluid viscosity

μ_t – fluid turbulent viscosity

$1:_{ij}$ – *ij*-th component of the laminar stress tensor

$1:^{R}_{ij}$ – *ij*-th component of the Reynolds stress tensor

Pr – the dimensionless Prandtl number

Pr_t – the dimensionless turbulent Prandtl number

C_p – fluid-specific heat capacity under constant pressure

T – temperature

x_i – *i*-th component of the Cartesian coordinate system

n_i – *i*-th component of the normal-to-the-wall in the fluid region

y – distance from the wall along the normal to it

y^+ – dimensionless distance from the wall along the normal to it

$1:_w$ – wall shear stress

q_w – heat flux from the wall to the fluid

K – the Karman factor

A_v – the Van Driest dumping factor

k_s – equivalent sand roughness height

β – boundary layer thickness calculated by the integral method

u^e – fluid velocity at the fluid boundary of the boundary layer

$1:^e_w$ – wall friction calculated by the integral method

a^e_w – heat flux from the wall to the fluid, calculated by the integral method

SUBSCRIPTS

l, *j*, *k* – directions of the Cartesian coordinate system

w – at the wall

+ – parameter is dimensionless on the basis of wall friction, fluid density, and fluid laminar viscosity